Competitive Inhibition of MAP Kinase Activation by a Peptide Representing the α_C Helix of ERK

Kurumi Y. Horiuchi,[‡] Peggy A. Scherle,[§] James M. Trzaskos,[§] and Robert A. Copeland*[,‡]

Chemical Enzymology and Inflammatory Diseases Research, The DuPont Merck Research Laboratories, P.O. Box 80400, Wilmington, Delaware 19880-0400

Received November 4, 1997; Revised Manuscript Received April 29, 1998

ABSTRACT: On the basis of the crystal structure of the MEK substrate ERK, we have synthesized a 15 amino acid peptide representing the α_C helix of human ERK1. We find this peptide to be an inhibitor of ERK phosphorylation by its upstream activator MEK. Circular dichroic spectroscopy indicates that the peptide has little secondary structure in aqueous buffer, but can readily adopt an α-helical structure in aprotic solvent. Steady-state kinetic analysis indicates that the peptide serves as a competitive inhibitor of ERK binding to MEK, with a dissociation constant, K_i, of 0.84 μM. Together with ATP-competitive inhibitors of MEK, we have used this peptide to define the kinetic mechanism of MEK catalysis. These studies reveal that MEK operates through a bi-bi random-ordered sequential mechanism. The synthetic peptide inhibits also the phosphorylation of p38 and ERK by the upstream activator MKK3, but is at least 3-fold less potent as an inhibitor of SEK activation of JNK1. Interestingly, the peptide also showed some ability to inhibit ERK-mediated phosphorylation of myelin basic protein, but was inactive as an inhibitor of the unrelated kinases Raf, Abl, and PKA. These results imply that the α_C helix is an important locus of interaction for the formation of a MEK−ERK complex. The α_C helix cannot, however, be the sole determinant of activator selectivity among the MAP kinases. Molecules designed to target the α_C helix binding pocket of MAP kinase activators may provide a novel means of inhibiting these signal transducers.

Signal transduction through the MAP kinase cascades induces transcriptional activation of a number of genes in response to stimuli such as growth factors, cytokines, osmotic shock, etc. (*1*). Among the genes activated through these cascades are several that have been linked to inflammatory diseases, autoimmune diseases, and certain forms of cancer. Selective inhibition of key components of the MAP kinase cascades therefore might serve as a basis for chemotherapeutic intervention in these diseases.

The crystal structure of one of the MAP kinases, ERK2, has been solved to atomic resolution (*2*). The structure (Figure 1) provides a detailed description of the atomic architecture of the enzyme. In vivo, ERK is activated through phosphorylation of both a threonine and tyrosine residue by the upstream kinase MEK (*3*). Recent studies of chimeras of MAP kinases have suggested that a domain containing, among other elements, an α helix referred to as the α_C helix (highlighted in Figure 1) may direct selectivity among the MAP kinases for their upstream activators (*4*). This helix, however, is distal to the activation loop of ERK, containing the threonine and tyrosine residues (highlighted in Figure 1) that are phosphorylated by MEK (*2*). Similarly, mutagenesis studies of other MAP kinases also suggest that structural elements distal to the activation loop play an important role in controlling MAP kinase specificity and enzymatic activity (*5, 6*). Surveying the crystal structure of human ERK2, one finds that the α_C helix is composed of the 15 amino acid sequence highlighted in Figure 1; by sequence homology, the α_C helix of the related MAP kinase ERK1 (*7*) is YCQRTLREIQILLRF.

On the basis of the ERK crystal structure and the previous studies of MAP kinase chimeras, we reasoned that a peptide representing the α_C helix of ERK1 might display selective inhibitory potency for the upstream activator MEK1. We therefore synthesized this 15 amino acid peptide, along with N- and C-terminally truncated peptides, and tested their abilities to serve as inhibitors of ERK activation by MEK. As expected, we find that the peptide serves as a competitive inhibitor of MEK with respect to the protein substrate ERK. We also have made use of this peptide-based inhibitor, along with competitive inhibitors of the ATP binding site of MEK, to define the kinetic mechanism of MEK catalysis. The results of these studies are presented here and indicate that MEK follows a bi-bi random ordered sequential mechanism.

MATERIALS AND METHODS

Materials. Expression and purification of the recombinant MAP kinases and their upstream activators (MEK1, ERK1, MKK3, p38, SEK, and JNK) will be described in a separate communication (Favata et al., manuscript in preparation). Bovine serum albumin (BSA), mastoparan, adensoine triphosphate (ATP), 5′-adenyl-imidodiphosphate (AMP−PNP), and buffer components (HEPES, TES, mercaptoethanol, and

* Corresponding author. Tel: (302) 695-7173. Fax: (302) 695-8313. E-mail: Robert.A.Copeland@Dupontmerck.com.
[‡] Chemical Enzymology.
[§] Inflammatory Diseases Research.

S0006-2960(97)02731-1 CCC: $15.00
Published on Web 06/05/1998

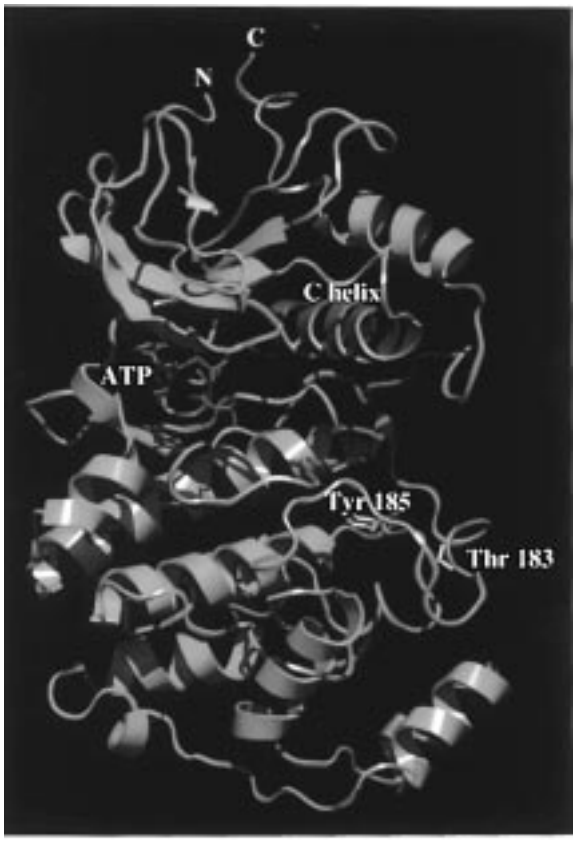

FIGURE 1: Ribbon diagram of the ERK2 structure highlighting the locations of the α_C helix (red), the bound ATP cofactor (blue), and the phophoacceptor residues threonine 183 and tyrosine 185 (both in yellow). The drawing was created using Quanta 96 from the atomic coordinates for rat brain ERK2, as described in ref *16*. This figure was kindly provided by Dr. Jodi Muckelbauer, DuPont Merck Research Laboratories.

$MgCl_2$) were purchased from Sigma. [γ-^{33}P]ATP was purchased from NEN. Peptides were custom synthesized by QCB (Cambridge, MA) with the N- and C-termini blocked as the acyl and amide forms, respectively. Each peptide was purified by reversed-phase HPLC, and its purity and identity were confirmed by mass spectral analysis. In all cases, the peptides used were of ≥95% purity. Acrylamide gels and buffers for electrophoresis were purchased from Novex and used according to the manufacturers instructions.

Enzyme Assays. In vitro assays of MEK phosphorylation of ERK were performed using constitutively active MEK1 (ΔN3/S218E/S222D; see ref *5* for further details) and a kinase-inactive mutant ERK1-GST construct (K71A; Favata et al., manuscript in preparation). For kinetic measurements that did not include the α_C peptide, the nitrocellulose filter binding assay described by Favata et al. (manuscript in preparation) was routinely used. We found, however, that at higher concentrations of peptide, the physical binding of ERK to the membranes was partially blocked, leading to an overestimation of the inhibition by the peptide. To avoid this complication, studies utilizing the α_C peptide were performed with either an electrophoretic gel based assay or an assay based of capture of the ERK-GST-fusion with glutathione-agarose on 0.22 μ filter plates. The electrophoretic gel assay was that described by Favata et al. (manuscript in preparation). Reactions were initiated by addition of ATP/[γ-^{33}P]ATP (1 mCi/μmol), and samples were removed after 0, 6, 12, and 18 min and mixed with 5× SDS reducing sample buffer to stop the reaction. Product formation was quantified by autoradiography after electrophoretic separation of the proteins in the reaction mixture.

The GST-capture assay was performed similarly. In this case, reactions were stopped by transferring the samples to wells of a 96-well 0.45 μ filter plate (Millipore) that contained enough 500 mM EDTA solution to make the final EDTA concentration 50 mM. Next 40 μL of a 50% (v/v) slurry of glutathione-agarose (Pharmacia) was added to each well, and the samples were incubated with constant agitation for 20 min at room temperature. After incubation, the membrane plate was evacuated and washed four times with 250 μL of PBS (phosphate buffered saline; Gibco) under vacuum. Wells were then filled with 30 μL of Microscint-20 (Packard) scintillation fluid, and the radioactivity of ^{33}P-phosphorylated ERK was counted with a Top Count (Packard) scintillation counter.

In all cases, product progress curves were linear over the entire 18 min reaction period, and the maximum amount of product formed was <4% of the total substrate concentration. Hence, initial velocities were determined from the slopes of the product progress curves by linear least-squares regression analysis. Reaction conditions were 10 mM $MgCl_2$, 0.1 mg/mL BSA, 10 mM β-mercaptoethanol, 20 mM HEPES (pH 7.4), and 10 nM MEK. Concentrations of ERK and ATP were varied over the ranges of 0.1−2.0 μM (0.2−4.8K_m) and 2.0−40.0 μM (0.3−7.2K_m), respectively. In most of the experiments described here the ERK and ATP concentrations were 400 nM and 40 μM, respectively, unless otherwise indicated.

MEK is a dual specificity kinase, capable of phosphorylating ERK at both tyrosine 185 and threonine 183 (*3*). In vitro studies by Haystead et al. (*25*) indicate, however, that ERK monophosphorylation at tyrosine 185 is the predominant product obtained under normal steady-state conditions. When these workers incubated ERK with 500 units of MEK and 200 μM ATP, they observed exclusively monophosphotyrosine 185 ERK as the product for up to 120 min of reaction. Only after complete exhaustion of the ATP substrate (180 min) did these workers detect any diphosphorylated ERK, and even under these extreme conditions, this product represented <1% of the total ERK present. No monophosphothreonine 183 ERK was detected by Haystead et al. under any conditions tested. On the basis of these results, with the lower ATP concentrations used and the limited substrate utilization under our conditions, we assume that the vast majority of the reaction being followed in our assays is the conversion of dephosphorylated ERK to monophosphotyrosine 185 ERK. Consistent with this assumption, the ERK K_m value reported here (0.42 ± 0.06 μM; see Table 3, vide infra) is similar to those reported by Mansour et al. (*26*) for an ERK2 mutant in which threonine 183 was replaced by an alanine (0.34−2.5 μM depending on the MEK form used). Further, we have confirmed by mass spectral analysis that only monophosphorylated ERK is formed over the first 20 min of reaction under the conditions used here, and have shown by Western blotting that this product is immunoreactive with a commerical (Santa Cruz Biotechnology) antiphosphotyrosine specific antibody (data not shown). Hence, we have analyzed our enzyme kinetic data by classical Henri-Michaelis−Menten analysis,

Table 1: Inhibiton of Various Kinases by the α_C Peptide

kinase	IC_{50} (μM)
MEK	4.6 ± 0.6
MKK3	4.2 ± 1.4
SEK	12.9 ± 1.1
ERK	14.4 ± 3.6
Raf	$>50^a$
Abl	$>50^a$
PKA	$>50^a$

[a] Less than 20% inhibition at the highest concentration tested (50 μM).

Table 2: Pattern of Product and Dead-End Inhibition of MEK

inhibitor	varied substrate	inhibition pattern
ADP	ATP	competitive
ADP	ERK	noncompetitive
AMP−PNP	ATP	competitive
AMP−PNP	ERK	noncompetitive
α_C helix peptide	ATP	noncompetitive
α_C helix peptide	ERK	competitive

Table 3: Apparent Kinetic Constants for MEK Turnover and Inhibition

kinetic constant[a]	value
k_{cat}	1.09 ± 0.06 min^{-1}
K_m-ATP	5.58 ± 1.00 μM
K_m-ERK	0.42 ± 0.06 μM
K_{ia} (ATP)	8.21 ± 2.13 μM
K_{ib} (ERK)	0.61 ± 0.18 μM
K_i-ADP	1.84 ± 0.07 μM
K_i-AMP-PNP	2.55 ± 0.24 μM
K_i-α_C helix peptide	0.84 ± 0.27 μM

[a] Kinetic constant nomenclature used here is that of Cleland (*24*).

assuming a single protein substrate (dephosphorylated ERK) and single protein product (monophosphotyrosine 185 ERK) for the enzyme. Nevertheless, we cannot exclude completely the possiblility that a small amount (less than detectable) of the monophosphotyrosine 185 ERK is converted to the diphosphorylated form during the course of our reactions. For this reason, we refer to the kinetic constants presented in Table 3 (vide infra) as *apparent* kinetic constants.

MKK3 activation of p38 was determined by an electrophoretic gel assay. Constitutively active GST-MKK3 and GST-p38 (Favata et al., manuscript in preparation) were incubated with [γ-^{33}P]ATP and various concentration of α_C peptide, and the level of ^{33}P-phosphorylation of GST-p38 was determined by autoradiography after SDS−PAGE. Conditions were similar to that of the MEK/ERK assay (vide supra), except that protein concentrations were 100 nM MKK3 and 300 nM p38.

The effect of the α_C peptide on SEK activation of JNK1 was also determined by an electrophoretic gel assay, similar to the method used for MKK3/p38 activation (vide supra). Proteins used for this study were all expressed in *Escherichia coli* (Favata et al., manuscript in preparation), and concentrations were 500 nM MEKK, 100 nM SEK, 400 nM JNK, and 2.5 μM Jun. The phosphorylation level of Jun was determined by autoradiography after SDS−PAGE. The effects of the α_C peptide on the kinase activities of Raf, ERK1/2, and Abl were studied using the assays describe by Favata et al. (manuscript in preparation). The ability of the α_C peptide to inhibit PKA was assessed using the Pierce

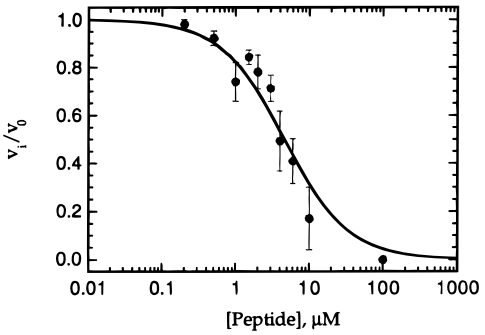

FIGURE 2: Concentration-dependent inhibition of MEK activity by the α_C helix peptide. Conditions were as described in the Materials and Methods. The line drawn through the data points represents the nonlinear least squares best fit to the Langmuir isotherm equation: $v_i/v_0 = 1/[1 + ([I]/IC_{50})]$, where v_i is the initial velocity in the presence of inhibitor at concentration [I], v_0 is the uninhibited initial velocity, and IC_{50} is the concentration of inhibitor that reduces the initial velocity to half of the uninhibited velocity (*11*).

colorimetric PKA assay kit (Product 29500) according to the suppliers instructions.

Steady-state velocity data were fit, by nonlinear curve-fitting methods, to the Henri-Michaelis−Menten equation to determine the values of the apparent K_m and V_{max} (*11*). These kinetic constants were then used to construct the lines drawn in the double reciprocal plots that are shown in the Results (*11*). Mode of inhibition for the various compounds used here was determined both from visual inspection of the double reciprocal plot patterns and by statistical comparisons of the best fits of the data to the appropriate equations for competitive, noncompetitive, and uncompetitive inhibition using the program Enzyme Kinetics (Ronald Viola, Akron, OH).

Circular Dichroic Spectroscopy. Circular dichroic (CD) spectra were obtained with a nitrogen-purged AVIV model 62 DS spectrometer. Scans from 250 to 185 nm were taken in 0.5 nm steps with a dwell time of 1 s/step. Samples (50 μM peptide in 10 mM TES buffer, pH 7.4 or in trifluoroethanol) were contained in 0.1 cm path length cuvettes. Each spectrum is the average of six scans and has had the appropriate solvent blank subtracted from it.

Secondary Structure Calculations. The secondary structure of the 15 residue α_C peptide was predicted with the program NNPREDICT, as described by Kneller et al. (*8*). The helical content of the peptide was calculated by deconvolution of the CD spectra using the method of Yang et al. (*9*).

RESULTS

Inhibition by the α_C Helix Peptide. A 15 amino acid peptide of the sequence YCQRTLREIQILLRF (referred to here as the α_C peptide; residues 1−15) was synthesized and tested in an in vitro assay of MEK phosphorylation of ERK. The peptide displayed a concentration-dependent inhibition of MEK which was well fit by the classical Langmuir isotherm equation (*11*), as illustrated in Figure 2. The IC_{50} (i.e., the concentration of inhibitor resulting in 50% inhibition) derived from nonlinear least-squares fitting of these data was 4.6 ± 0.6 μM. To ensure that the inhibitory effects observed here were specific to the sequence of the α_C helix peptide, we tested a 14 amino acid peptide of unrelated sequence, mastoparan, which is known to form α-helical

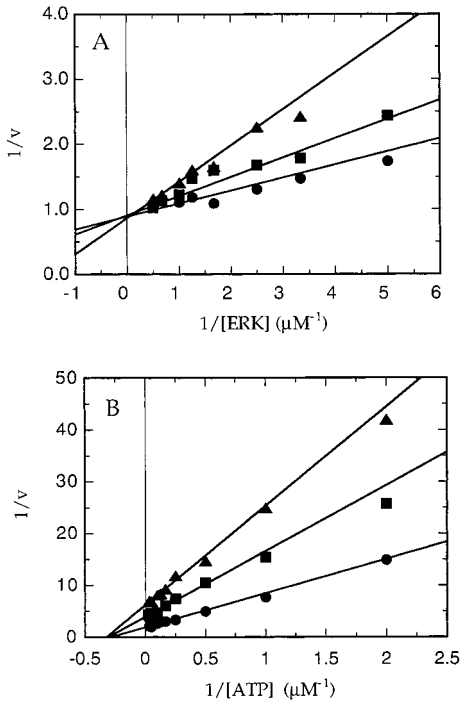

FIGURE 3: Effects of α_C peptide on MEK-mediated phosphorylation of ERK. (A) Lineweaver−Burk plot for the inhibition of MEK activity by the α_C helix peptide at varying concentrations of ERK. Concentrations of α_C helix peptide used were 0 (circle), 1.5 (square), and 3 μM (triangle). (B) Lineweaver−Burk plot for the inhibition of MEK activity by the α_C helix peptide at varying concentrations of ATP. Symbols are the same as in panel A.

structure under certain conditions (*10*), and a scrambled peptide with the same amino acid composition as the α_C helix peptide, of sequence QLFRLYCQRLIETIR. Neither of these peptides displayed any inhibition of ERK phosphorylation by MEK at concentrations as high as 100 μM.

To determine the minimum sequence required to effect MEK inhibition, we also had synthesized two 10 amino acid peptides representing 5 amino acid truncations from the N- and C-termini of the α_C-helix peptide, respectively. The C-terminally truncated peptide,YCQRTLREIQ (residues 1−10), was ineffective as a MEK inhibitor at concentrations as high as 100 μM. The N-terminally truncated peptide, LREIQILLRF (residues 6−15), displayed reduced inhibitory potency, shifting the IC_{50} for MEK inhibition to 9.1 ± 2.2 μM. These results suggest that the C-terminal region of the peptide may play a dominant role in peptide binding to MEK, but that the entire 15 residue sequence of the α_C helix peptide is required for optimal MEK binding and inhibition.

To determine the mode of MEK inhibition by the α_C helix peptide, steady-state kinetic analysis was performed (Figure 3). The pattern of double reciprocal plots (*11*) indicate that the peptide is competitive with respect to ERK (a nest of lines converging at the *y*-axis of the double reciprocal plot; Figure 3A) and noncompetitive with respect to ATP (a nest of lines converging below zero on the *x*-axis; Figure 3B). An alternative explanation for these results is that the peptide acts as an alternate substrate for MEK, rather than a true competitive inhibitor. To explore this possibility we tested whether the peptide could be phosphorylated by MEK in our standard assay, but in the absence of ERK. No ^{33}P-incorporation into the peptide could be detected, indicating that it does not function as a MEK substrate.

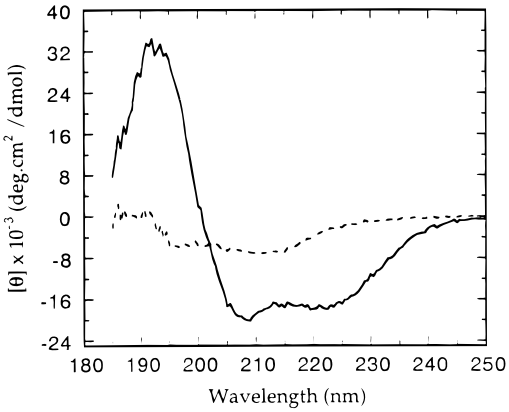

FIGURE 4: Circular dichroic (CD) spectra of the α_C helix peptide in aqueous solution (10 mM TES, pH 7.4; dashed line) or in trifluoroethanol (solid line).

The untransformed data used to construct Figure 3A were globally fit to the equation for competitive inhibition (*11*) from which the K_i value for the α_C-helix peptide was determined to be 0.84 ± 0.27 μM.

Secondary Structure of the α_C Helix Peptide. The 15 residue peptide used here was designed from a known α-helical segment of the ERK protein. Secondary structure calculations predict that eight of the residues within this 15-mer (53%) have a high propensity for α-helix formation (*8*). To determine if the synthetic peptide was helical under the assay conditions for ERK phosphorylation by MEK, we measured the far ultraviolet circular dichroic (CD) spectrum (*12*) of the peptide (Figure 4). In aqueous buffer, the peptide shows a paucity of secondary structure, which is not uncommon for peptides of this size. When, however, the peptide is dissolved in the aprotic solvent trifluoroethanol, the CD spectrum dramatically changes to one reflecting a high content (53%) of α-helical secondary structure (*9*). Hence, the peptide is indeed capable of adopting a helical structure under appropriate solution conditions. Whether or not the peptide is helical when bound to MEK could not be determined from the present study. We note, however, that there are many examples of peptides of this size that adopt an α-helical structure when bound to their target protein; the peptides mellitin and mastoparan, for example, are known to become helical upon complex formation with calcium-replete calmodulin (*13*).

Specificity of the α_C Helix Peptide toward MAP Kinase Kinases. To assess the specificity of the α_C-helix peptide as a MAP kinase kinase inhibitor, we tested its ability to inhibit the kinase activity of EKR, MKK3, SEK, and the unrelated kinases Raf, Abl, and PKA (Table 1). The α_C-helix peptide showed good inhibitory potency for blocking MKK3 activation of p38, with an IC_{50} of 4.2 ± 1.4 μM. Interestingly, in the course of these studies, we found that MKK3 was not only capable of phosphorylating p38, but also phosphorylated ERK, albeit to a lesser extent (about 8% of the velocity observed with p38 as substrate). This very modest rate of ERK phosphorylation by MKK3 is unlikely to be of any physiological significance. Nevertheless, given this apparent permissiveness of MKK3, it may not be surprising that the α_C-helix peptide can also inhibit this MAP kinase kinase. The other MAP kinase kinase tested was SEK. Here, we see about a 3-fold reduction in inhibitory potency (IC_{50} = 12.9 ± 1.1 μM) for the α_C peptide relative

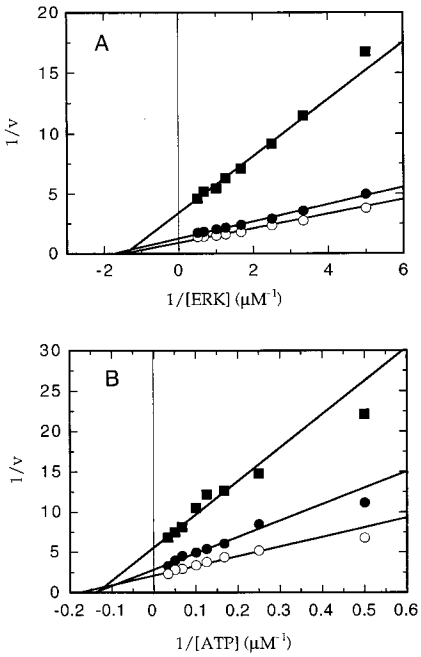

FIGURE 5: Two-substrate kinetic analysis of MEK. (A) Double reciprocal plot for velocity as a function of ERK concentration at several fixed concentrations of ATP. The ATP concentrations used were 2 (closed squares), 10 (closed circles), and 30 μM (open circles). (B) Double reciprocal plot for velocity as a function of ATP concentration at several fixed concentrations of ERK. The ERK concentrations used were: 0.1 (closed squares), 0.4 (closed circles), and 1.0 μM (open circles).

to its potency as an inhibitor of MEK. In separate experiments, we determined that, unlike MEK and MKK3, SEK was unable to phosphorylate ERK to any detectable level (data not shown). The peptide also showed some activity as an inhibitor of ERK-mediated phosphorylation of myelin basic protein ($IC_{50} = 14.4 \pm 3.6$ μM). In contrast, the α_C peptide was completely inactive as an inhibitor of the unrelated kinases Raf, Abl, and PKA.

Kinetic Mechanism of MEK Catalysis. The α_C-helix peptide is a competitive inhibitor of MEK with respect to ERK binding. Hence, together with competitive inhibitors of ATP binding, this peptide provides a unique tool for determining the kinetic mechanism of MEK-catalyzed phosphorylation of ERK.

To determine the kinetic mechanism of MEK catalysis, we first varied the concentrations of both substrates, ATP and ERK, and determined the effects of these changes on reaction velocity. Figure 5 illustrates the double reciprocal plots for $1/v$ as a function of 1/[ERK] at varying fixed ATP concentration and $1/v$ as a function of 1/[ATP] at varying fixed ERK concentrations, respectively. For both plots, the lines drawn through the data points converge to the left of the *x*-axis origin. This pattern of nonparallel, converging lines rules out a ping-pong mechanism for MEK, and instead indicates a bi-bi sequential kinetic mechanism. Hence, the two substrates form a ternary complex with MEK prior to product release. The order of substrate addition to the enzyme may be random or compulsory, the data in Figure 5 being insufficient to distinguish between these possibilities.

Having ruled out a ping-pong kinetic mechanism for MEK, we next sought to differentiate between a random and compulsory ordered sequential mechanism. For this purpose, we investigated the pattern of inhibition brought about by the product of phosphate transfer, ADP, and by a nonhydrolyzable ATP analogue, AMP−PNP. Both of these compounds are structurally related to the substrate ATP and should bind to MEK at its ATP-binding site. Until now, there were no inhibitors known for MEK that were competitive with ERK binding. As described in the previous section (vide supra), however, the α_C helix peptide acts as a competitive inhibitor of MEK with respect to the substrate ERK. The pattern of inhibition seen for this peptide and for the two ATP analogues, when either ATP or ERK was the varied substrate, are presented in Table 2. For both ADP and AMP−PNP one observes competitive inhibition for ATP and noncompetitive inhibition for ERK. For the peptide inhibitor, one observes competitive inhibition with respect to ERK and noncompetitive inhibition with respect to ATP (see also Figure 3). None of these inhibitors showed any evidence of uncompetitve inhibition with respect to the alternative substrate for MEK. These data are consistent with a random order of substrate addition to the enzyme. With this kinetic mechanism established, we have fit the data presented in Figure 5 to the appropriate equation for a bi-bi random ordered sequential mechanism (*11*) and have thus determined the kinetic parameters listed in Table 3 for MEK.

DISCUSSION

Activation of ERK requires two phosphorylation events, both of which are carried out by the upstream activator, MEK. It has recently been determined that the dual phosphorylation of ERK by MEK occurs in a nonprocessive fashion, requiring release and rebinding of the monophosphorylated ERK molecule from MEK (*17, 18*). The kinetic mechanism for interaction between MEK, ERK, and ATP was not, however, defined until now. Our ability to define the kinetic mechanism of MEK was greatly aided by the availability of a competitive inhibitor with respect to ERK binding, the α_C-helix peptide. The kinetic data presented here demonstrate that MEK follows a bi-bi random ordered sequential kinetic mechanism. This result is consistent with the kinetic mechanisms reported for a number of other protein kinases (*19*−*22*). In contrast, LoGrasso et al. (*23*) recently reported that p38 MAP kinase follows a bi-bi compulsory ordered sequential mechanism in which the protein substrate binds before ATP. These authors pointed out that their studies utilized a protein substrate for p38 MAP kinase, while previous studies of protein tyrosine kinases used peptide-based substrates and suggested that this difference might account for the apparent disparity in kinetic mechanisms. The present data, however, suggest that utilization of a protein substrate cannot account for the difference in kinetic mechanism observed by LaGrasso et al. Like these workers, we too have used a protein substrate for our present studies. Hence, the differences in mechanism between p38 MAP kinase and MEK most likely are inherent to these enzymes and not a result of the substrate used in the in vitro assays. Why these related signal transducing kinases function by different kinetic mechanisms is not clear at this time.

Referring to Tables 2 and 3, we note that the product ADP is a competitive inhibitor of MEK with respect to the substrate ATP. That this product demonstrates competitive inhibition indicates the formation of a dead-end ternary complex, MEK·ADP·ERK. From Table 3 we see that the

Scheme 1

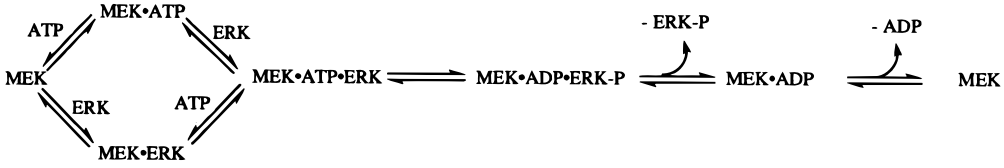

affinity for ADP and the nonhydrolyzable ATP analogue AMP−PNP are of similar magnitude to that of the substrate ATP; in fact, these compounds display slightly greater affinity for MEK. Taken together these results suggest that ADP release from MEK is slow and may be the rate-limiting step in MEK turnover. If this inference is correct, then the mechanism of MEK turnover would involve random addition of substrates, but ordered release of products with ADP being the last product to leave, as illustrated in Scheme 1.

While speculative, the ordered product release illustrated in Scheme 1 would be consistent with the nonprocessive nature of the dual phosphorylation of ERK by MEK, as recently described by Ferrell and Bhatt (*17*). These workers demonstrated that dual phosphorylation of ERK requires release and subsequent rebinding of monophosphorylated ERK to MEK. A mechanism such as that suggested here, that is rate limited by ADP release from the enzyme, would facilitate rapid release of monophosphorylated (and perhaps diphosphorylated)-ERK from the enzyme. What the relative MEK affinities and off rates are for these varied ERK forms is an unresolved issue; this would need to be addressed through rapid kinetic studies to fully elucidate the mechanism of MEK turnover.

The MAP kinase chimera studies of Brunet and Pouyssegur (*4*) indicated that, at least in cellular assays, the activator selectivity of MAP kinases is dictated by a region between domains III and V, containing the α_C helix, loops L5 and L6, and two strands of β-pleated sheet, β_4 and β_5. Because the α_C helix is the only one of these structural elements that is clearly surface exposed in the crystal structure of ERK2, it seemed reasonable to expect that this helix would play a major role in activator binding and selectivity. While the present results support a role for this helix in binding to the upstream activators of MAP kinases, the selectivity, with respect to other MAP kinase cascade members, demonstrated in our in vitro assays is modest at best. Hence, contrary to our expectation, it appears that the α_C helix alone is insufficient to act as the sole determinant of MAP kinases activator selectivity. It is also interesting to note that the α_C peptide was also a modest inhibitor of ERK activity (Table 1). This result suggests that the α_C helix of ERK not only participates in upstream activator binding, but may also play a role in binding of substrates to ERK.

We have demonstrated that the α_C peptide binds to MEK with affinity ($K_i = 0.84\ \mu$M; Table 3) similar to that of the full ERK molecule ($K_{ib} = 0.61\ \mu$M; Table 3) and competitively blocks ERK phosphorylation by MEK. This result is somewhat surprising in that the α_C helix is clearly distant from the loop containing the phosphoaccepting tyrosine and threonine residues of ERK (see Figure 1). Complexation between MEK and ERK must occur in such a way as to bring into close proximity the phosphoaccepting residues of ERK and the catalytic active site of MEK. Thus, the α_C-helix portion of the ERK molecule must interact with a binding site on the MEK molecule that is distinct from the catalytic active site; the current results suggest that this interaction accounts for a significant portion of the overall binding free energy for intermolecular complexation. Indeed, preliminary experiments indicate that the α_C helix peptide can completely block the physical binding of MEK1 to immobilized GST-ERK1 (Horiuchi and Copeland, unpublished results). In contrast, attempts to design peptide-based substrates of MEK, based on the sequence of the phosphoacceptor-containing loop, have not been successful (*15*), possibly because structural determinants distal to this loop play an important role in MEK−ERK binding. Additionally, recent studies of ERK mutations within this loop region support the idea that other regions of the ERK molecule are important in determining the affinity and selectivity of MAP kinases for their upstream activators (*5*, *6*). The present results suggest that the α_C helix may be an important locus on ERK for MEK binding, consistent with the chimera studies of Brunet and Pouyssegur (*4*).

Taken together, these results imply that substrate binding and catalysis are facilitated by separate and distinct structural determinants within the MEK protein. This suggested segregation of substrate-binding elements and catalytic machinery for the MAP kinases may be an extreme example of the *split-site* model of enzyme catalysis proposed by Menger (*14*). In an attempt to rationalize the competing needs for ground-state substrate binding and transition-state stabilization by enzymes, this model suggests that the loci for substrate binding and the elements that produced ground-state distortions of the substrate constitute separate structural features of the enzyme active site. In the case of the MAP kinases, where the substrate is a macromolecular protein, this partitioning of substrate binding and enzyme catalysis may have reached the ultimate situation where the structural determinants of substrate binding are distal to the actual active site of phosphorylation. Hence, active-site directed distortions of the substrate ground-state structure may occur after substrate binding, perhaps in concert with a more global conformational rearrangement of the enzyme molecule, as has been suggested for the MAP kinases (*1*). Thus, as seen in this report, targeting of the substrate-binding site, rather than the enzyme active site per se, may be an alternative approach to the design of competitive inhibitors of the MAP kinases and other enzymes that act upon macromolecular substrates.

ACKNOWLEDGMENT

We thank Wendi Feeser for the MAP kinase constructs used in this study, Karl Blom for mass spectral analysis of our samples, and Jodi Muckelbauer for providing the structural model of ERK presented in Figure 1.

REFERENCES

1. Goldsmith, E. J., and Cobb, M. H. (1994) *Curr. Opin. Struct. Biol. 4*, 833−840.

2. Zhang, F., Strand, A., Robbins, D., Cobb, M. H., and Goldsmith, E. J. (1994) *Nature 367*, 704−711.
3. Anderson, N. G., Maller, J. L., Tonks, N. K., and Sturgill, T. W. (1990) *Nature 343*, 651−653.
4. Brunet, A., and Pouysse'gur, J. (1996) *Science 272*, 1652−1655.
5. Mansour, S. J., Candia, J. M., Matsuura, J. E., Manning, M. C., and Ahn, N. G. (1996) *Biochemistry 35*, 15529−15536.
6. Robinson, M. J., Cheng, M., Khokhlatchev, A., Ebert, D., Ahn, N., Guan, K.-L., Stein, B., Goldsmith, E., and Cobb, M. H. (1996) *J. Biol. Chem. 271*, 29734−29739.
7. Boulton, T. G., Nye, S. H., Robbins, D. J., Ip, N. Y., Radziejewska, E., Morgenbesser, S. D., DePinho, R. A., Panayotatos, N., Cobb, M. H., and Yancopoulos, G. D. (1991) *Cell 65*, 663−675.
8. Kneller, D. G., Cohen, F. E., and Langridge, R. (1990) *J. Mol. Biol. 214*, 171−182.
9. Yang, J. T., Wu, C.-S. C., and Martinez, H. M. (1986) *Methods Enzymol. 130*, 208−269.
10. Nakajima, T., Yasuhara, T., Uzu, S., Wakamatsu, K., Miyazawa, T., Fukuda, K., and Tsukamoto, Y. (1985) *Peptides 6*, 425−430.
11. Copeland, R. A. (1996) *Enzymes: A Practical Introduction to Structure, Mechanism, and Data Analysis*, pp 93−119, Wiley-VCH, New York.
12. Copeland, R. A. (1994) *Methods for Protein Analysis: A Practical Guide to Laboratory Protocols*, pp 191−197, Chapman & Hall, New York.
13. Clore, G. M., Bax, A., Ikura, M., and Gronenborn, A. M. (1993) *Curr. Opin. Struct. Biol. 3*, 838−845.
14. Menger, F. M. (1992) *Biochemistry 31*, 5368−5373.
15. Seger, R., Ahn, N. G., Posada, J., Munar, E. S., Jensen, A. M., Cooper, J. A., Cobb, M. H., and Krebs, E. G. (1992) *J. Biol. Chem. 267*, 14373−14381.
16. Zhang, J., Zhang, F., Ebert, D., Cobb, M. H., and Goldsmith, E. J. (1995) *Structure (London) 3*, 299−307.
17. Ferrell, J. E., and Bhatt, R. R. (1997) *J. Biol. Chem. 272*, 19008−19016.
18. Burack, W. R., and Sturgill, T. W. (1997) *Biochemistry 36*, 5929−5933.
19. Cook, P. F., Neville, M. E., Jr., Vrana, K. E., Hartl, T., and Roskoski, R., Jr. (1982) *Biochemistry 21*, 5794−5799.
20. Posner, I., Engel, M., and Levitzki, A. (1992) *J. Biol. Chem. 267*, 20638−20647.
21. Cole, P. A., Burn, P., Takacs, B., and Walsh, C. T. (1994) *J. Biol. Chem. 269*, 30880−30887.
22. Boener, R. J., Barker, S. C., and Knight, W. B. (1995) *Biochemistry 34*, 16419−16423.
23. LoGrasso, P. V., Frantz, B., Rolando, A. M., O'Keefe, S. J., Hermes, J. D., and O'Neill, E. A. (1997) *Biochemistry 36*, 10422−10427.
24. Cleland, W. W. (1979) *Methods Enzymol. 63*, 103−138.
25. Haystead, T. A. J., Dent, P., Wu, J., Haystead, C. M. M., and Sturgill, T. W. (1992) *FEBS Lett. 306*, 17−22.
26. Mansour, S. J., Candia, J. M., Matsuura, J. E., Manning, M. C., and Ahn, N. G. (1996) *Biochemistry 35*, 15529−15536.

BI972731Q